Mechanism of Propene–Deuterium Addition and Exchange Reaction over Silica-Supported ZrO_2

Shuichi NAITO* and Mitsutoshi TANIMOTO†
Department of Applied Chemistry, Faculty of Engineering, Kanagawa University,
3-27-1, Rokkakubashi, Kanagawa-ku, Yokohama 221
† Department of Chemistry, Faculty of Science, Shizuoka University, 836 Ohya, Shizuoka 422
(Received July 20, 1994)

The mechanism of propene–deuterium reaction over unsupported and silica-supported ZrO_2 catalysts was studied with kinetic investigation as well as microwave spectroscopic analysis of monodeuteriopropene. Unsupported ZrO_2 exhibited the identical catalytic behavior for C_3H_6–D_2 reaction with other oxide catalysts previously reported: Only propane-d_2 was selectively formed in the addition process, with no hydrogen exchange in propene. By supporting on silica, the rate of C_3H_6–D_2 reaction increased considerably, with the decrease of activation energy. Hydrogen exchange in propene proceeded simultaneously with addition via associative mechanism through propyl and isopropyl intermediates. Small particles of ZrO_2 were proposed as active sites of this characteristic catalytic behavior.

The activity and the selectivity of the catalytic reaction over supported metal catalysts greatly depend on the particle size of the metal and the nature of the support material.[1] Morphological change of the metal with particle sizes and its electronic interaction with the support may be the main factors governing these phenomena.[2,3] Such effect for supported metal oxide catalysts has not so far been investigated in detail. Recently we have shown that highly dispersed metal oxides (TiO_2, ZnO, and ZrO_2) on various supports such as SiO_2, Al_2O_3, and TiO_2 exhibit remarkably different catalytic behavior in propene–deuterium addition and exchange reactions.[4,5] However, its detailed mechanism and the nature of active sites have not been clarified yet.

Two different mechanisms have been proposed for the hydrogen addition and exchange reactions of propene over metal and metal oxide catalysts. Their difference is most markedly recognized in the hydrogen-exchange process. Over metal catalysts, in the presence of gaseous hydrogen, the reaction proceeds exclusively through σ-alkyl intermediates, propyl and isopropyl adsorbed species (associative mechanism).[6—8] Hydrogen exchange of propene takes place by the reverse reaction of this process. In the absence of hydrogen gas, the reaction proceeds through dissociated intermediates, i.e., 1- and isopropenyl and σ- and π-allyl adsorbed species.

On the other hand, over metal oxide catalysts, the reverse process of σ-alkyl intermediate formation is prohibited or at most negligibly slow in comparison with the addition process.[9—14] Accordingly, in the C_3H_6–D_2 reaction, a single deuterium molecule maintains its molecular identity in the addition process to form only $C_3H_6D_2$, and no hydrogen exchange of propene takes place through associative mechanism. The exchange process, if it proceeds, takes place through a completely different mechanism independent of the addition process.

In the present investigation, we studied C_3H_6–D_2 and C_3H_6–C_3D_6 reactions over unsupported and silica-supported ZrO_2 catalyst and found that catalytic behavior of zirconium oxide changed remarkably by supporting it on silica and resembled that of metal catalysts. Combined use was made of an isotopic tracer technique and microwave spectroscopy to elucidate the mechanistic difference over these catalysts. Microwave spectroscopy can locate the D atom in the exchanged propene-d molecule and thus clarify the structure of the reaction intermediates adsorbed on the catalysts.[15] In the C_3H_6–D_2 reaction, relative reactivity of propyl and isopropyl intermediates may be estimated from the isotope distributions. Accordingly, this technique enables us to determine how the particle sizes of supported oxides affect the reaction rates and the reaction intermediates.

Experimental

The experimental procedures are described in our previous publications.[7,8] We briefly mention the preparation of the catalysts and the reaction procedure.

Supported ZrO_2 catalyst was prepared by an impregnation method using SiO_2 powder (Aerosil 300), evacuated at 723 K for 2 h, and dry hexane solution of $Zr(OC_3H_7{}^i)_4$ (Soegawa Chemicals) under nitrogen atmosphere. The catalyst was oxidized by O_2 at 923 K overnight. Small amount of water was added to the hexane solution of $Zr(OC_3H_7{}^i)_4$ to obtain unsupported ZrO_2 catalyst. Binding energy of Zr in the catalyst was measured with an XPS spectrometer, ESCALAB-5, using Mg $K\alpha$ as an X-ray source. For the calibration of the binding energies, $Au4f_{7/2}$ (84.0 eV) was used as a reference.

Hydrogen and deuterium gases from commercial cylinders were purified over a heated Pd black catalyst to remove trace amount of oxygen. C_3H_6 (Takachiho Kagaku K.K.), C_3D_6, and $H_2C{=}CD{-}CH_3$ (Merck, Sharp and Dohme Ltd.) were purified by a freeze-thaw cycle. 1-Propene-1-d ($HDC{=}CH{-}CH_3$) was prepared from 1-bromo-1-propene.[16]

Before each run the catalyst (ca. 1 g) was freshly oxidized by O_2 at 623 K for 2 h, followed by an evacuation at the same temperature for 30 min. A mixture of the reaction gases was introduced into the system after cooling down to the reac-

tion temperature. A few percent of the circulating gas was sampled at certain intervals and separated into propane and propene by gas chromatography (alumina column, He carrier). The deuterium contents were determined with a mass spectrometer (Hitachi RMU-6MG). The amount of various monodeuteriopropene was determined by recording the microwave absorption line (1_{01}–0_{00} rotational transition). The isotopomers were denoted as follows:

cis-1-propene-*d* : 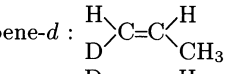

trans-1-propene-*d* : 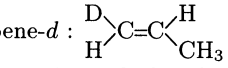

1-propene-2-*d* : $H_2C{=}CD{-}CH_3$

1-propene-3-*d* : $H_2C{=}CH{-}CH_2D$

Results

Kinetics of C_3H_6–D_2 Reaction. A mixture of C_3H_6 (3.4 kPa) and D_2 (26.7 kPa) reacted at 423 K on unsupported ZrO_2 catalyst. Propane was the only reaction product and no hydrogen exchange of propene took place as shown in Fig. 1(a). Figure 2(a) shows that most of the formed propane incorporated two D atoms. At the beginning, small amount of nondeuterated propane was formed, which decreased rapidly as the reaction proceeded.

Completely different result was obtained in the case of 8 wt% ZrO_2/SiO_2 catalyst, as shown in Fig. 1(b). Both deuterium addition and exchange of propene proceeded simultaneously. Propane and propene-*d* were main products at the initial stage, which suggested a stepwise reaction in the hydrogen-exchange process. The isotope distribution pattern in propane is shown in Fig. 2(b), where nondeuterated propane was initially the main product, Propane-*d*, -d_2, etc. gradually increased in amount, as the reaction proceeded. At the later stage, propane-d_2 was the main product. The mechanism of the initial formation of nondeuterated propane is not clear at present; self-hydrogenation of propene or rapid dilution of surface D (from gaseous D_2) by surface H (from hydroxide) may be occurring at the beginning of the reaction.

Table 1 gives the initial rates and the activation energies of deuterium addition and exchange processes over various catalysts investigated in this study. Initial rate of propene-*d* formation over silica-supported ZrO_2 catalysts was twice as fast as that of propane formation. However, the activation energies are same for both processes, which strongly suggests that they proceed via associative mechanism through the same σ-alkyl reaction intermediates. The dependence of the initial rate of propane formation in the C_3H_6–D_2 reaction upon the amount of ZrO_2 loaded on silica is also summarized in the table. At lower loading (up to 16 wt%), the specific rate was independent of the amount of ZrO_2 loaded, suggesting that the particle size of ZrO_2 supported on silica remains unchanged. On the other hand, the propane formation was considerably slower over unsupported ZrO_2 than over supported ZrO_2, and its activation energy (53 kJ mol^{-1}) was significantly higher.

Pressure dependence of the C_3H_6–D_2 reaction rate over unsupported and 8 wt% silica-supported ZrO_2 catalysts was summarized in Fig. 3. Over unsupported catalyst, the reaction orders were 0.52 and zero with respect to the partial pressures of hydrogen and propene, respectively. This result suggests that the rate-determining step on unsupported ZrO_2 is the addition of the first hydrogen atom to the double bond carbon of adsorbed propene forming a propyl intermediate. The

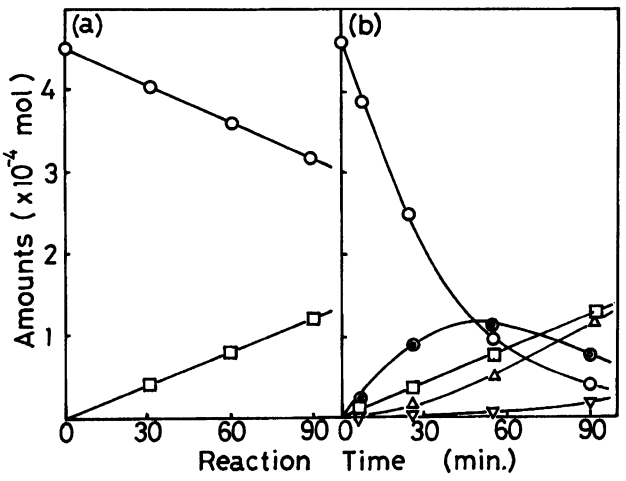

Fig. 1. Time courses of the C_3H_6–D_2 reaction at 423 K (a) over unsupported ZrO_2 and (b) over 8 wt% ZrO_2/SiO_2. Catalysts=1 g. P_{C3H6}=3.4 kPa, P_{D2}=26.7 kPa. ○: C_3H_6, ◎: C_3H_5D, △: $C_3H_4D_2$, ▽: $C_3H_3D_3$, □: Propane.

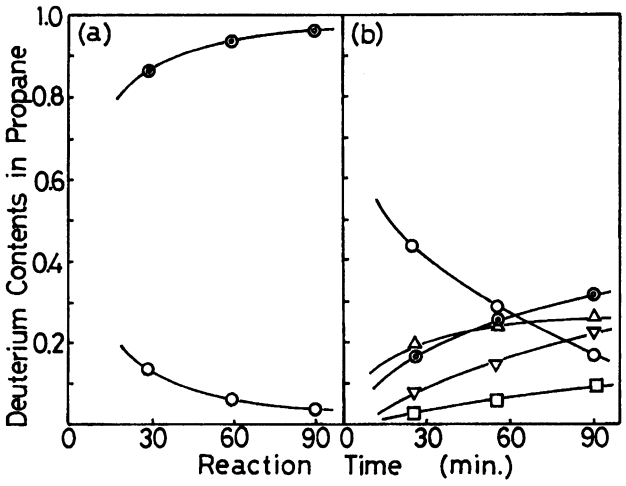

Fig. 2. Time courses of deuterium contents in propane formed during the C_3H_6–D_2 reaction at 423 K (a) over unsupported ZrO_2 and (b) over 8 wt% ZrO_2/SiO_2. Catalysts=1 g. P_{C3H6}=3.4 kPa, P_{D2}=26.7 kPa. ○: C_3H_8, △: C_3H_7D, ◎: $C_3H_6D_2$, ▽: $C_3H_5D_3$, □: $C_3H_4D_4$.

Table 1. Initial Rates and Activation Energies of C_3H_6–D_2 and C_3H_6–C_3D_6 Reactions over Various Catalysts

Reaction and Catalysts	Reac. temp	Initial rates $\times10^{-7}$ mol s^{-1} g-ZrO_2^{-1}		Activation energy[c] kJ mol^{-1}	
	K	Addition	Exchange	Addition	Exchange
C_3H_6–D_2[a]					
Unsupported ZrO_2	423	0.3	—	53	—
ZrO_2/SiO_2 1 wt%	423	4.0	7.8	39	39
2 wt%	423	4.0	7.8		
4 wt%	423	3.9	7.7		
8 wt%	423	3.8	7.6	40	40
16 wt%	423	3.5	7.1		
C_3H_6–C_3D_6[b]					
Unsupported ZrO_2	473		0.1		76
ZrO_2/SiO_2 1 wt%	473		0.7		
8 wt%	473		0.6		75

a) $P_{D2}=3.4$ kPa, $P_{C3H6}=26.7$ kPa. b) $P_{C3H6}=P_{C3D6}=1.7$ kPa. c) Activation energies were obtained from the Arrhenius plots of the initial rates at the temperature range of 380—530 K.

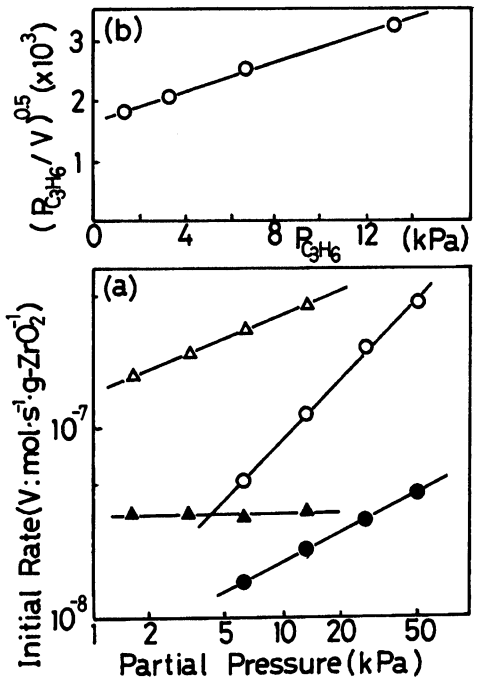

Fig. 3. (a) Pressure dependence of the initial rate of propane formation upon the partial pressures of H_2 and C_3H_6 at 423 K. Open symbols: 8 wt% ZrO_2/SiO_2 (1 g), Closed symbols: unsupported ZrO_2 (1 g), ○ ●: P_{H2} dependence ($P_{C3H6}=3.4$ kPa constant) △ ▲: P_{C3H6} dependence ($P_{H2}=26.7$ kPa constant). (b) Plots of the values $(P_{C3H6}/V)^{0.5}$ versus P_{C3H6} over 8 wt% ZrO_2/SiO_2.

reverse process of this step (hydrogen abstraction from propyl species) did not occur, since no hydrogen exchange was observed during the reaction. By supporting on silica, the reaction orders became larger: 1.0 for the partial pressure of hydrogen and 0.38 for propene, suggesting the change of the rate-determining step to the introduction of a second hydrogen into the propyl intermediate.

Dispersed State of ZrO_2 on Silica. The XPS results of various catalysts (Table 2) show that on dispersing, $Zr3d_{5/2}$ peaks shifted about 1.0 eV toward higher binding energy, suggesting a certain electronic interaction of dispersed ZrO_2 with the supports. Assuming that XPS intensity was proportional to the surface area (relative intensity ratio of the peaks Zr/Si=8.54), we estimated the atomic ratio of Zr/Si on the surface from the corrected peak areas of Zr3d and Si2s emissions. The atomic ratio given in Table 2 is far smaller than the value expected for the monoatomic overlayer of ZrO_2 on silica (1.0). The dispersion of ZrO_2, D_{Zr}, is calculated with the following equation:

$$D_{Zr}=\frac{(Zr)_s}{(Zr)_b}=\frac{(Zr)_s}{(Si)_s}\times\frac{(Si)_b}{(Zr)_b}\times\frac{(Si)_s}{(Si)_b},$$

where suffixes denote s=surface and b=bulk. The last factor $(Si)_s/(Si)_b$ is estimated from the observed average diameter of silica particles=70 Å. If we assume that spherical particles of ZrO_2 and silica should contact each other in these catalysts, the values of dispersion in the table indicate that very small particles (15—20 Å diameter) are formed on silica and that their sizes are independent of the loaded amount of ZrO_2 up to 8 wt% catalyst.

Table 2. Dispersion of ZrO_2 on Silica by XPS

Catalysts/wt%	$Zr3d_{5/2}$ B.E./eV	Zr/Si Surface	Zr/Si Bulk	Dispersion D
Unsupported ZrO_2	182.6			
ZrO_2/SiO_2 1.0	183.7	0.0088	0.0044	0.53
8.0	183.5	0.064	0.042	0.45
50.0	183.1	0.306	0.485	0.19

Isotope Distribution in C_3H_6–D_2 and C_3H_5D–H_2 Reactions. Figure 4 demonstrates the temporal change in the isotope distribution of monodeuteriopropenes formed during the C_3H_6–D_2 reaction over 1 and 8 wt% ZrO_2/SiO_2 catalysts. If the exchange process proceeds through the σ-alkyl intermediates alone, the rate of 1-propene-2-*d* formation (from propyl species) and those of 1-propene-1-*d* and 3-*d* formation (from isopropyl species) remain unaltered at the initial stage of the reaction. Considerable change in the isotope distribution may result from an intramolecular hydrogen shift process. This process should be independent of the deuterium incorporation process through the associative mechanism.

To confirm this intramolecular isomerization mechanism, 1-propene-1-*d*+H_2 and 1-propene-2-*d*+H_2 reactions were carried out under the conditions similar to that of Fig. 4. A large isotope ratio of H to D (10 : 1) in the present system makes deuterium exchange by the repetition of σ-alkyl intermediates negligible. The results are shown in Fig. 5(a) and (b). When only 1-propene-1-*d* was introduced on 8 wt% ZrO_2/SiO_2 catalyst at 423 K, the decrease of 1-propene-1-*d* was accompanied by the increase of 1-propene-3-*d* (closed symbols). When H_2 was added to this system, hydrogen exchange was accelerated, with the accompanied formation of propane. The situation was different in the case of 1-propene-2-*d*+H_2 reaction, where no exchange was observed in the absence of H_2, as shown in Fig. 5-(b) (closed symbol). These results clearly indicate the existence of intramolecular 1,3- as well as 2,3-hydrogen shift processes during the C_3H_6–D_2 reaction in Fig. 4.

Dependence of the distribution pattern of the C_3H_6–D_2 reaction upon the amount of ZrO_2 loading is illustrated in Fig. 6. Initial isotope distribution was estimated by extrapolating the observed composition (Fig. 4) into time zero. Over 1 wt% catalyst, the amount of 1-propene-1-*d* (68%) exceeded that of 2-*d* (32%). As the ZrO_2 loading increases, the ratio of 1-*d* (58%) to 2-*d* (42%) reaches a constant value. This observation is consistent with the findings from dispersion value that the particle size of ZrO_2 on silica support does not change much with the loaded amount.

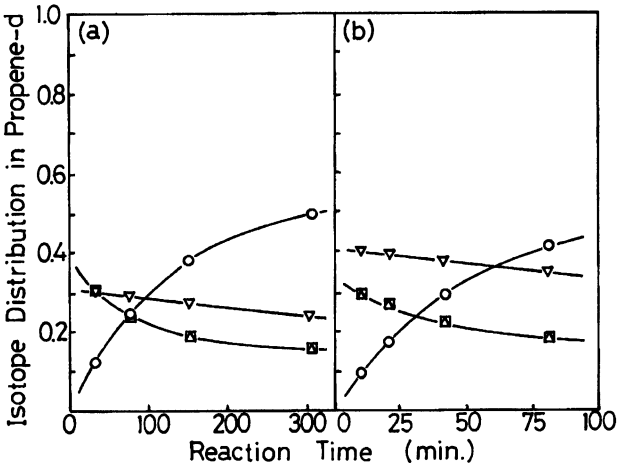

Fig. 4. Time courses of the isotope distribution in propene-d_1 formed during the C_3H_6–D_2 reaction at 423 K (a) over 1 wt% ZrO_2/SiO_2 and (b) over 8 wt% ZrO_2/SiO_2. Catalysts=1 g. P_{C3H6}=3.4 kPa, P_{D2}=26.7 kPa. □: *cis*-1-propene-*d*, △: *trans*-1-propene-*d*, ▽: 1-propene-2-*d*, ○: 1-propene-3-*d*.

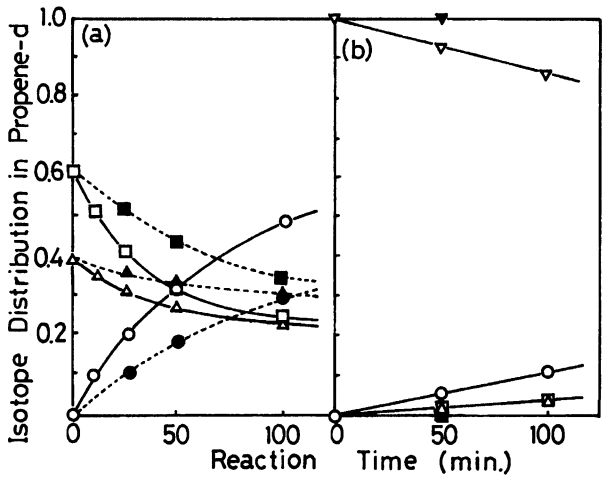

Fig. 5. Time courses of the isotopic distribution in propene-*d* during the C_3H_5D–H_2 reaction ((a) 1-propene-1-*d*+H_2 and (b) 1-propene-2-*d*+H_2) over 8 wt% ZrO_2/SiO_2 at 423 K. Open symbols with solid lines: C_3H_5D–H_2 reaction (P_{C3H5D}=3.4 kPa and P_{H2}=26.7 kPa), closed symbols with broken lines: C_3H_5D only (P_{C3H5D}=3.4 kPa), □: *cis*-1-propene-*d*, △: *trans*-1-propene-1-*d*, ▽: 1-propene-2-*d*, ○: 1-propene-3-*d*.

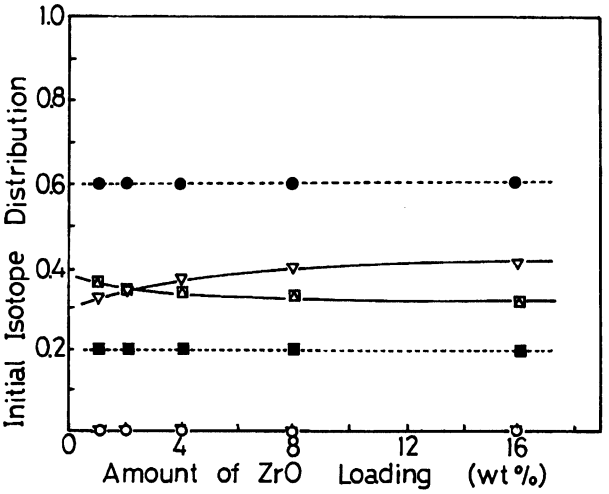

Fig. 6. Dependence of the initial isotope distribution of the C_3H_6–D_2 (423 K: solid lines, P_{C3H6}=3.4 kPa, P_{D2}=26.7 kPa) and C_3H_6–C_3D_6 (503 K: broken lines, $P_{C3H6}=P_{C3D6}$=1.7 kPa) reactions upon the amount of ZrO_2 loaded on SiO_2. Catalysts=1 g. □: *cis*-1-propene-1-*d*, △: *trans*-1-propene-1-*d*, ▽: 1-propene-2-*d*, ○: 1-propene-3-*d*.

C_3H_6–C_3D_6 Reaction. When a mixture of C_3H_6 and C_3D_6 (1 : 1, 1.7 kPa each) was admitted onto unsupported ZrO_2 and 8 wt% ZrO_2/SiO_2 catalysts at around 500 K, intermolecular hydrogen-exchange reaction of propene readily proceeded. The rate was one order of magnitude slower than the intramolecular 1,3-hydrogen shift process. The main products at the initial stage were almost the same amount of C_3H_5D (propene-d) and C_3HD_5 (propene-d_5), as shown in Fig. 7(a) and (b). The amount of highly exchanged propene was very small, indicating a stepwise exchange in the reaction between propene molecules. The initial rate of propene-d formation as well as the activation energy were listed in Table 1. Both catalysts have the same activation energy, 75—76 kcal mol^{-1}, for this intermolecular hydrogen-exchange process.

The position of deuterium in monodeuteriopropene was determined with microwave spectroscopy, the result being displayed in Fig. 8. The isotopic distribution patterns on both catalysts were almost identical: 60% of 1-propene-3-d and 40% of 1-d (equal amount of cis and trans isomers). Since the intramolecular hydrogen shift process proceeds more than one order of magnitude faster than the intermolecular process, the observed patterns should reflect exchange equilibrium between methyl and methylene hydrogens after the incorporation of deuterium into propene through intermolecular C_3H_6–C_3D_6 reaction. Under these circumstances, it is rather difficult to distinguish a carbonium cation type intermediate from dissociated ones like 1-propenyl and σ- or π-allyl adsorbed species.

The dependence of the initial rates of monodeuteriopropene formation as well as its isotope distribution pattern was summarized in Table 1 and Fig. 6. At lower loading (up to 8 wt%), the rate was proportional to the amount of ZrO_2, which is identical with the case of the C_3H_6–D_2 reaction.

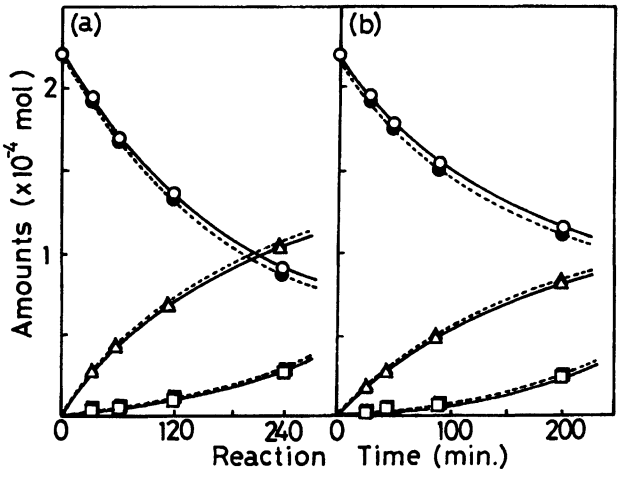

Fig. 7. Time courses of the C_3H_6–C_3D_6 reaction (a) over unsupported ZrO_2 at 473 K and (b) over 8 wt% ZrO_2/SiO_2 at 503 K. Catalysts=1 g. $P_{C3H6}=P_{C3D6}=1.7$ kPa. ○: C_3H_6, △: C_3H_5D, □: $C_3H_4D_2$, ■: $C_3H_2D_4$, ▲: C_3HD_5, ●: C_3D_6.

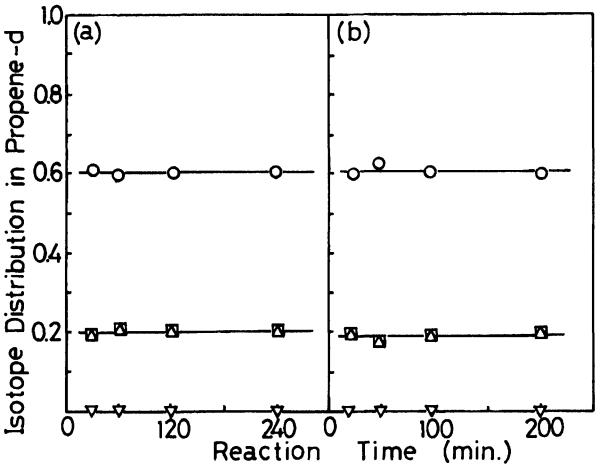

Fig. 8. Time courses of the isotope distribution in 1-propene-d during the C_3H_6–C_3D_6 reaction (a) over unsupported ZrO_2 at 473 K and (b) over 8 wt% ZrO_2/SiO_2 at 503 K. Catalysts=1 g. $P_{C3H6}=P_{C3D6}=1.7$ kPa. □: *cis*-1-propene-1-d, △: *trans*-1-propene-1-d, ▽: 1-propene-2-d, ○: 1-propene-3-d.

Discussion

Unique character of metal oxide catalysts has been reported for the hydrogenation of ethene over Cr_2O_3,[9] ZnO,[10,11] and Co_3O_4,[12] and for 1,3-butadiene over ZnO[13] and MgO.[14] In these reactions, both H (or D) atoms in a hydrogen molecule are incorporated into a single hydrogenated molecule, retaining molecular identity. Accordingly, in the reaction between olefin and D_2, dideuterated paraffin is the main product, which is produced through either of the two different reaction mechanisms: One-step addition of a deuterium molecule or two-step addition of deuterium atoms to a C=C bond.

The mechanism of the hydrogenation of ethene over ZnO was examined in detail by Dent and Kokes[17,18] by applying kinetic studies supplemented with infrared techniques. The initial rate of ethane formation was proportional to square root of the hydrogen pressure and only slightly dependent on ethene pressure. By infrared spectroscopic observation of adsorbed species during the reaction, the rate-determining step was concluded to be the insertion of adsorbed ethene into Zn–H bond to form Zn–ethyl intermediate. The reverse process of this step seemed to be prohibited, because no hydrogen exchange of ethene took place. To elucidate the molecular identity of added hydrogen atoms, an isolated Zn–O ion pair with surrounding lattice O^{2-} was postulated to be the active site.

In the present study over unsupported ZrO_2, the experimental rate equation was: $V=kP_{H2}{}^{0.5}P_{C3H6}{}^{0}$, which was very similar to that of ZnO. Hence, isolated Zr–O ion pairs may be the active site also for propene hydrogenation and the following reaction schemes can

be proposed for the C_3H_6–D_2 reaction over unsupported catalyst.

$$H_2 + Zr\text{–}O \rightleftharpoons H\text{–}Zr\text{–}O\text{–}H \quad \text{step (1)}$$

$$C_3H_6 + (O^{2-}) \rightleftharpoons C_3H_6\text{–}(O^{2-}) \quad \text{step (2)}$$

$$Zr\text{–}H + C_3H_6\text{–}(O^{2-}) \rightarrow Zr\text{–}C_3H_7 + (O^{2-}) \quad \text{step (3)}$$

$$Zr\text{–}C_3H_7 + O\text{–}H \rightarrow Zr\text{–}O + C_3H_8 \quad \text{step (4)}$$

Here, Zr–O represents an isolated Zr^{2+} and O^{2-} ion pair, which is surrounded by lattice oxygen (O^{2-}). To derive the reaction orders with respect to the partial pressures of hydrogen and propene, we have to assume that their adsorption sites are independent of each other. Moreover, adsorption of hydrogen on Zr–O should be weak, whereas that of propene on (O^{2-}) strong. The concentrations of adsorbed hydrogen atoms and propene molecules are then proportional to $P_{H2}{}^{0.5}$ and $P_{C3H6}{}^{0}$, respectively. The rate-determining step would be step (3), and the following rate equation can be derived from the scheme:

$$V = k[Zr\text{–}H][C_3H_6\text{–}(O^{2-})] = k'P_{H2}{}^{0.5}P_{C3H6}{}^{0}. \quad \text{(I)}$$

Since hydrogen exchange of propene did not proceed on unsupported catalysts, the reverse process of step (3) should be prohibited, which may be explained by the inactivity of lattice (O^{2-}) for the abstraction of hydrogen atom from $Zr\text{–}C_3H_7$.

By supporting ZrO_2 on silica, the situation changed completely, and hydrogen exchange of propene proceeded concomitantly with the addition process. This implies that the reverse process of step (3) is now accessible, suggesting the structural transformation of active sites on ZrO_2 surface as a result of supporting. To clarify this point, we attempted to vary the particle sizes of ZrO_2 on silica by changing the amount of loading and to examine its influence upon the reaction rates as well as the reaction mechanism. As demonstrated in Table 1, the initial formation rate of propane in the C_3H_6–D_2 reaction as well as that of monodeuteriopropene in the C_3H_6–C_3D_6 reaction were proportional to the amount of ZrO_2 loading on silica at the lower loading regions (1—10 wt%), which suggested that the particle size of ZrO_2 prepared on silica support was similar and independent of the amount loaded. This was confirmed by the estimation of dispersion from XPS data (Table 2).

It has been reported that ZrO_2 with small particle size is obtained by thermolysis of zirconium tetraalkoxides.[19] The structure of amorphous ZrO_2 has been investigated in detail by Livage et al.[20] using electron microscopy and small-angle X-ray scattering. They proposed a two-dimensional model, that is, a thin plate consisting of one layer of Zr atoms between two oxygen layers (diameter: 20—60 Å, thickness: 4—6 Å). It seems reasonable to suppose that such thin plates of ZrO_2 would be formed also when it is supported on silica. If we assume that hydrogen atoms can move around on this two-dimensional network of zirconium and oxygen overlayers, the following reaction scheme may be applicable, where both hydrogen and propene molecules are adsorbed on the common surface vacant site, S:

$$H_2 + 2S \overset{K_1}{\rightleftharpoons} 2H_S \quad \text{step (5)}$$

$$C_3H_6 + S \overset{K_2}{\rightleftharpoons} C_3H_{6S} \quad \text{step (6)}$$

$$C_3H_{6S} + H_S \overset{K_3}{\rightleftharpoons} C_3H_{7S} + S \quad \text{step (7)}$$

$$C_3H_{7S} + H_S \overset{k_4}{\longrightarrow} C_3H_8 + 2S \quad \text{step (8)}$$

In the above scheme, a species with suffix S is a surface-adsorbed species. K_1—K_3 represent the equilibrium constants of the corresponding steps, and k_4 the rate constant of the forward reaction of step (8). If we assume that step (8) is the rate-determining step, the following rate equation is derived from the scheme:

$$V = k_4K_1K_2K_3P_{H2}P_{C3H6}/\{1 + (K_1P_{H2})^{0.5} + K_2P_{C3H6}\}^2. \quad \text{(II)}$$

Pressure dependence shown in Fig. 3(a) yields the following experimental rate equation: $V = kP_{H2}{}^{1.0}P_{C3H6}{}^{0.38}$. Because of first order in the partial pressure of hydrogen, the equilibrium constant K_1 (H_2 adsorption) should be negligibly small, which is an acceptable assumption under the present reaction condition. In the experiments carried out with constant P_{H2}, Eq. II can be rewritten as follows:

$$(P_{C3H6}/V)^{0.5} = \alpha P_{C3H6} + \beta \quad (\alpha, \beta : \text{constants}) \quad \text{(III)}$$

In Fig. 3(b), the values of $(P_{C3H6}/V)^{0.5}$ are plotted against P_{C3H6}. Since they form a straight line, the reaction scheme (5)—(8) is recognized to be applicable to the C_3H_6–D_2 reaction over ZrO_2/SiO_2 catalysts.

Hydrogen exchange of propene proceeds by the reverse process of step (7), which is faster than the hydrogen addition process (step (8)). Isotope distribution pattern of monodeuteriopropene indicates that deuterium incorporation takes place only at double bond carbons C_1 and C_2, and methyl hydrogens are inactive for exchange by this process. Independently of the above exchange process, 1,3- and 2,3-intramolecular hydrogen shift processes are present, which cause a methyl hydrogen to exchange to form 1-propene-3-*d*. Inactivity of methyl group for hydrogen exchange via associative mechanism may be explained by a large steric hindrance of an oxygen overlayer on top of a Zr layer, which causes a distorted adsorption of isopropyl intermediate.

On the other hand, little effect of supporting was observed for the C_3H_6–C_3D_6 reaction over these catalysts. The isotope distribution pattern does not contain sufficient information to speculate on the structure of the reaction intermediates in this process. The exchange rate over supported ZrO_2 is much faster than that of unsupported catalyst, whereas the activation energies are

identical over these catalysts. Accordingly it is appropriate to suppose that both unsupported and supported catalysts possess the same reaction sites for the C_3H_6–C_3D_6 reaction, and their amount is more abundant on supported catalysts than on unsupported one.

References

1) M. Boudart, *Adv. Catal.*, **20**, 153 (1969).
2) M. Boudart, *J. Mol. Catal.*, **30**, 27 (1985).
3) G. A. Somorjai and J. Carrazza, *Ind. Eng. Chem. Fundam.*, **25**, 63 (1986).
4) S. Naito and M. Tanimoto, *Chem. Lett.*, **1990**, 2145.
5) S. Naito, M. Tanimoto, and M. Soma, *J. Chem. Soc., Chem. Commun.*, **1992**, 1443.
6) J. Horiuti and M. Polanyi, *Trans. Faraday Soc.*, **30**, 1164 (1934).
7) S. Naito and M. Tanimoto, *J. Catal.*, **102**, 337 (1986).
8) S. Naito and M. Tanimoto, *J. Chem. Soc., Faraday Trans. 1*, **83**, 2475 (1987).
9) M. Carwell and R. L. Burwell, Jr., *J. Am. Chem. Soc.*, **82**, 6289 (1969).
10) W. C. Conner, R. A. Innes, and R. J. Kokes, *J. Am. Chem. Soc.*, **90**, 6858 (1968).
11) W. C. Conner and R. J. Kokes, *J. Phys. Chem.*, **73**, 2436 (1969).
12) A. Ozaki and T. Fukushima, *J. Catal.*, **37**, 561 (1975).
13) S. Naito, Y. Sakurai, H. Shimizu, T. Onishi, and K. Tamaru, *Bull. Chem. Soc. Jpn.*, **43**, 2274 (1970); *Trans. Faraday Soc.*, **67**, 1529 (1971).
14) Y. Hattori, Y. Tanaka, and K. Tanabe, *J. Am. Chem. Soc.*, **98**, 4652 (1976).
15) T. Kondo, S. Saito, and K. Tamaru, *J. Am. Chem. Soc.*, **96**, 6857 (1974).
16) W. P. Norris, *J. Org. Chem.*, **24**, 1579 (1959).
17) A. L. Dent and R. J. Kokes, *J. Am. Chem. Soc.*, **91**, 7207 (1969).
18) A. L. Dent and R. J. Kokes, *J. Phys. Chem.*, **73**, 3772 and 3781 (1969).
19) K. S. Mazdiyasni, C. T. Lynch, and J. S. Smith, *J. Am. Ceram. Soc.*, **49**, 286 (1966).
20) J. Livage, K. Doi, and C. Mazieres, *J. Am. Ceram. Soc.*, **51**, 349 (1968).